Analytical Biochemistry 528 (2017) 19–25

Contents lists available at ScienceDirect

Analytical Biochemistry

journal homepage: www.elsevier.com/locate/yabio

Fabrication of electrochemical biosensor with vanadium pentoxide nano-interface for the detection of methylglyoxal in rice

Lakshmi Priyankka Alagappan [a, b, 1], Preethi Shanmugasundaram [a, b, 1], Bhat Lakshmishri Ramachandra [a, c], Manju Bhargavi Gumpu [a, c], Noel Nesakumar [a, b], K. Jayanth Babu [a, c], Srinivasan Vedantham [a, b], John Bosco Balaguru Rayappan [a, c, *]

[a] Centre for Nanotechnology & Advanced Biomaterials (CeNTAB), SASTRA University, Thanjavur 613 401, Tamil Nadu, India
[b] School of Chemical & Biotechnology, SASTRA University, Thanjavur 613 401, Tamil Nadu, India
[c] School of Electrical & Electronics Engineering, SASTRA University, Thanjavur 613 401, Tamil Nadu, India

ARTICLE INFO

Article history:
Received 13 September 2016
Received in revised form
17 January 2017
Accepted 18 April 2017
Available online 23 April 2017

Keywords:
Methylglyoxal
Reduced glutathione
Vanadium pentoxide nanoparticle
Bioelectrode
Rice

ABSTRACT

Increased consumption of raw and par-boiled rice results in the formation of methylglyoxal (MG) at higher concentration and leads to complications in diabetic patients. Highly sensitive electrochemical biosensor was developed using glutathione (GSH) as a co-factor with vanadium pentoxide (V_2O_5) as a nano-interface for MG detection in rice samples. The Pt/V_2O_5/GSH/Chitosan bioelectrode displayed two well-defined redox peaks in its cyclic voltammograms for MG reduction. This occurred as two electron transfer process where MG gained two electrons from oxidized glutathione disulfide and formed hemithioacetal. The current density response of the fabricated bioelectrode was linear towards MG in the concentration range of 0.1–100 μM with the correlation coefficient of 0.99, sensitivity of 1130.86 μA cm^{-2} μM^{-1}, limit of detection of 2 nM and response time of less than 18 s. The developed bioelectrode was used for the detection of MG in raw and par-boiled rice samples.

Introduction

Rice is a staple food source for nearly half of the world's population [1]. Rice has higher levels of methylglyoxal (MG) than other foods [2]. Increase in the consumption of rice elevates the glucose level, which results in the formation of MG in higher concentration and leads to complications in diabetic patients [3–5]. MG is pathologically related to macro and micro angiopathy, hypertension, insulin resistance, vascular damage and age-related complications [6–8]. The normal MG concentration is around 0.1–0.7 μM in human plasma, whereas the MG concentration in type -I and type -II diabetes is 7–8.4 μM and 2.8–4.2 μM respectively [3]. Hence, an efficient analytical method is required for the determination of MG in rice.

Ion pair chromatography, gas chromatography, high performance liquid chromatography, mass spectrometry, capillary electrophoresis and Enzyme Linked Immuno Sorbent Assay (ELISA) are the various conventional methods being used to detect MG. But, these techniques are time consuming, require extensive and expensive sample preparation and trained personnel [3,9,10]. Due to specific advantages, such as simplicity, high specificity, sensitivity, rapid response time and low cost, electrochemical biosensors have been developed for the detection of MG. MG detection is done *via* both enzymatic [11] and non-enzymatic modes of detection [3,9,10,12,13]. From previous investigations, it is noted that most of the researchers worked on non-enzymatic biosensors [3,9,10,12,13]. Single walled carbon nanotubes (SWCNTs) and nano-platinum (Pt) are the nanomaterials used so far to electrocatalyze the conversion of MG to hemithioacetal [9,10]. However, lack of specificity is the major drawback in using these nanomaterials as electrocatalysts [9,10]. To overcome the specificity issue, enzymatic biosensor based on glyoxalase I (GLO 1) enzyme was preferred. Thangavel et al. [12] and Ezhilan et al. [13] developed MG biosensors by modifying Pt electrode with zinc oxide (ZnO) nanosepals and nanoflakes for the detection of MG in human blood serum and grilled chicken respectively. Though ZnO nanoflakes and nanosepals enhanced the electron transfer rate between GLO 1 enzyme and Pt electrode, the inability of these modified bioelectrodes to generate

* Corresponding author. Centre for Nanotechnology & Advanced Biomaterials (CeNTAB) & School of Electrical & Electronics Engineering, SASTRA University, Thanjavur 613 401, India.
E-mail address: rjbosco@ece.sastra.edu (J.B. Balaguru Rayappan).
[1] Both authors have contributed equally in this work.

http://dx.doi.org/10.1016/j.ab.2017.04.010
0003-2697/

hemithioacetal makes them inferior [12,13]. In order to overcome these drawbacks, Ramachandra et al. [3] developed an electrochemical biosensor by immobilizing GLO 1 on Pt/CeO_2 bioelectrode in which the immobilized GLO 1 enzyme catalyzed MG to hemithioacetal and later to S-D lactoylglutathione in the presence of glutathione (GSH) as cofactor. Though the GLO 1 based electrochemical MG sensors are highly specific in nature, high cost of GLO 1 enzyme makes them unsuitable for large scale industrial production [3]. Owing to the low cost of GSH and the ability of GSH to convert MG to hemithioacetal, GSH based electrochemical MG biosensor has been preferred in this investigation.

Like ZnO and CeO_2 nanoparticles, vanadium pentoxide (V_2O_5) nanoparticles have attracted researchers in the fabrication of bioelectrodes owing to their high catalytic property, high electron transfer rate and good biocompatibility [14–20]. V_2O_5 nanoparticles have an isoelectric point of 3, which can immobilize GSH cofactor with high isoelectric point of 5.93 through electrostatic attraction and prevent leaching of GSH [21]. In this work, a reliable electrochemical biosensor based on GSH modified Pt/V_2O_5 electrode has been fabricated to detect MG in rice samples using cyclic voltammetry technique.

Materials and methods

Materials

L-glutathione-reduced was purchased from Hi-Media, India. MG was obtained from Sigma-Aldrich, USA. All other chemicals such as sodium hydroxide pellets purified, sucrose, dibasic sodium phosphate, lactic acid, monobasic sodium phosphate, glucose, chitosan, ascorbic acid and urea were purchased from Merck India Ltd., India. Ammonium metavanadate was purchased from Nice - chemicals Pvt. Ltd., Kerala, India. All the reagents and solutions were prepared using double de-ionized water (Aqua purification system, India).

Synthesis of V_2O_5 nanoparticles

0.05 M of ammonium metavanadate (NH_4VO_3) precursor solution was prepared by dissolving 0.87 g of NH_4VO_3 in 150 mL of deionized water. Then the solution was stirred continuously for 35 min at room temperature to obtain the pale yellow coloured solution. Later, the solution was kept in microwave oven at 180 W for 75 min. Finally, the dried form of dark brown coloured V_2O_5 nanoparticles was collected. The microwave irradiation helped in dissociation of agglomerated particles through heating effect by dipolar polarization and conduction process. The heating effect on the molecules lead to collision of particles resulting in the formation of smaller particles. The chemical reaction of formation of V_2O_5 from ammonium metavanadate is as follows:

$$2\ NH_4VO_3 \rightarrow V_2O_5 + 2\ NH_3 + H_2O$$

Fabrication of Pt/V_2O_5/GSH/Chitosan bioelectrode

Chitosan of 10 μL (0.25 wt%) was added to 1 mg of V_2O_5 nanoparticles and the solution was sonicated for 15 min. Later, 5 μL of GSH (100 μM) was added to the above solution, which was further sonicated for 1 min. Then, 3 μL of the sonicated product was taken and drop-casted on the Pt electrode's surface. Finally, the Pt electrode was allowed to dry at room temperature for 7 h.

Characterization techniques

The morphologies of Pt/V_2O_5, V_2O_5/GSH, Pt/V_2O_5/GSH/Chitosan bioelectrodes were observed using field emission scanning electron microscope (FE-SEM, Model JSM 6701F, JEOL, Japan). The structural property of V_2O_5 nanoparticles was studied using X-ray diffractometer (D8 Focus, Bruker, Germany). The immobilization of chitosan and GSH on V_2O_5 nanointerface was confirmed using Fourier transform infrared spectrometer (FTIR, Model Spectrum 100, Perkin Elmer, USA).

Electrochemical analysis

Electrochemical measurements were performed using an electrochemical workstation (CH1600C, CH Instrument, USA). The three electrode system comprised of Pt/V_2O_5/GSH/Chitosan as a working electrode, Ag/AgCl saturated with 0.1 M KCl as a reference electrode and platinum wire as an auxiliary electrode was used to carry out the experiment. All cyclic voltammetric experiments were performed in a 20 mL electrochemical cell with 5 mL PBS (0.1 M, pH 7.4) solution at room temperature in the potential range of −0.3 to 0.4 V (*vs Ag/AgCl*).

Preparation of real sample

Raw rice and par-boiled rice samples were purchased from local market and the rice samples were grounded. Later, grounded rice samples of 1 mg was taken and homogenized with 10 μL of PBS (0.1 M, pH 7.4). This mixture was sonicated for 10 min. Finally, under the optimal experimental conditions, recovery study was carried out by spiking known amount of MG to homogenized rice samples.

Results and discussion

Morphological studies

The morphologies of V_2O_5, V_2O_5/GSH and V_2O_5/GSH/Chitosan are shown in Fig. 1(a–c). The morphologies of V_2O_5 and V_2O_5/GSH were in the form of agglomerated arabic gum whereas the V_2O_5/GSH/Chitosan showed smooth agglomerated featureless morphology. In order to highlight the successful formation of V_2O_5 nanoparticles and their composite with GSH and chitosan, FE-TEM analysis was performed. The FE-TEM image of the synthesized V_2O_5 nanoparticles revealed the cuboid-like morphology with a mean height of 210 nm and a mean length of 228 nm (Fig. 1(d)). On adding GSH to the V_2O_5 nanoparticles (Fig. 1(e)), there was an increase in mean height of the nanoparticles around 12 nm with a size ranging from 190 to 254 nm. It confirmed immobilization of GSH on the surface of V_2O_5 nanoparticles. On adding chitosan membrane to V_2O_5/GSH, an agglomerated globular morphology was observed (Fig. 1(f)).

XRD characterization of nanostructured V_2O_5 sample

X-ray diffraction pattern (Cu K α radiation source1.54 Å) of the as-prepared V_2O_5 nanoparticles is shown in Fig. 2(a). For the nanostructured V_2O_5 sample, the diffraction peaks were obtained at 2θ = 18.07°, 23.77°, 27.18°, 8.25°, 30.71°, 33.02°, 34.01°, 35.63°, 36.56°, 38.86°, 40.71°, 42.71°, 43.78°, 45.01°, 46.24°, 47.48°, 49.32°, 51.01°, 53.01°, 56.55°, 61.01°, 63.16°, 63.93° corresponding to (200), (001), (101), (110), (400), (011), (310), (211), (401), (111), (002), (102), (401), (411), (141), (600), (012), (020), (601), (021), (320), (710), (711) planes, which confirmed the orthorhombic structure of V_2O_5 nanoparticles according to Joint Committee on Powder

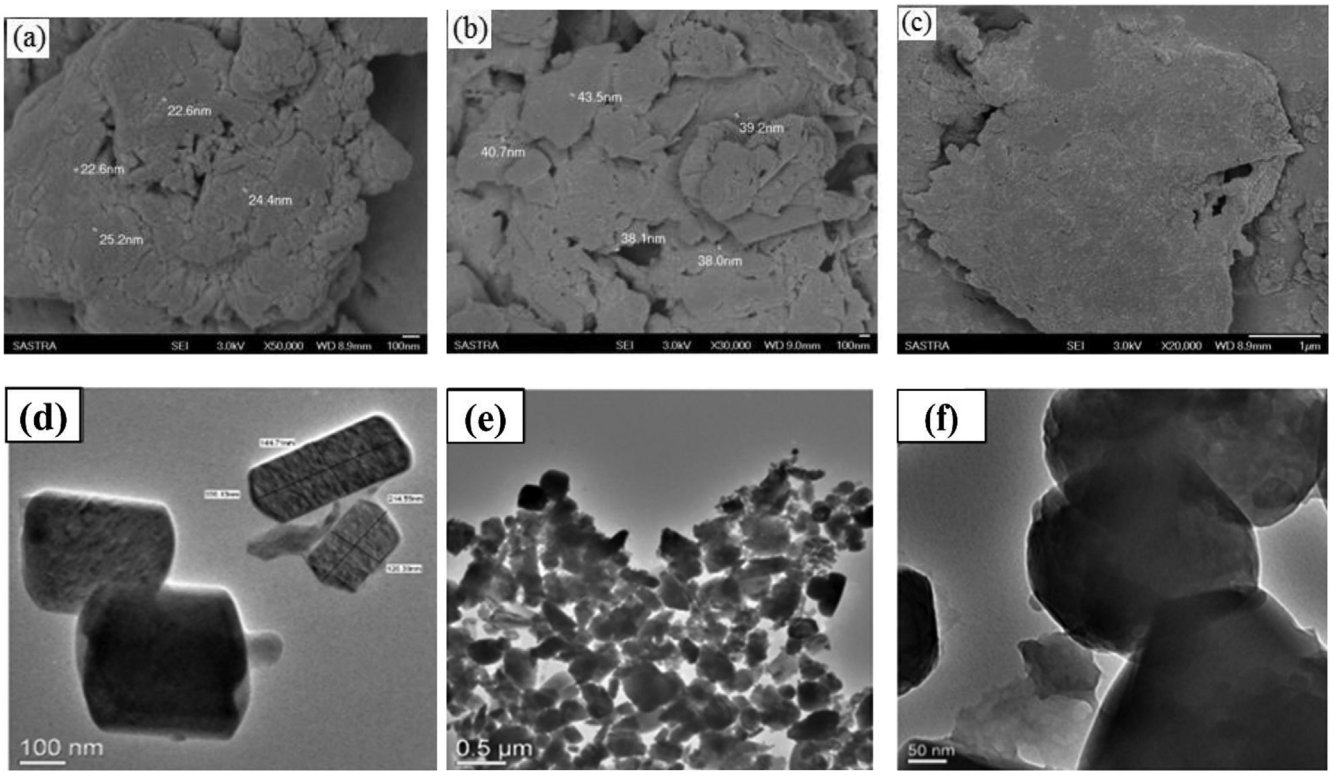

Fig. 1. FE-SEM images of the as-prepared (a) V_2O_5 nanoparticles, (b) V_2O_5/GSH, (c) V_2O_5/GSH/Chitosan and FETEM images of (d) V_2O_5 nanoparticles, (e) V_2O_5/GSH and (f) V_2O_5/GSH/Chitosan.

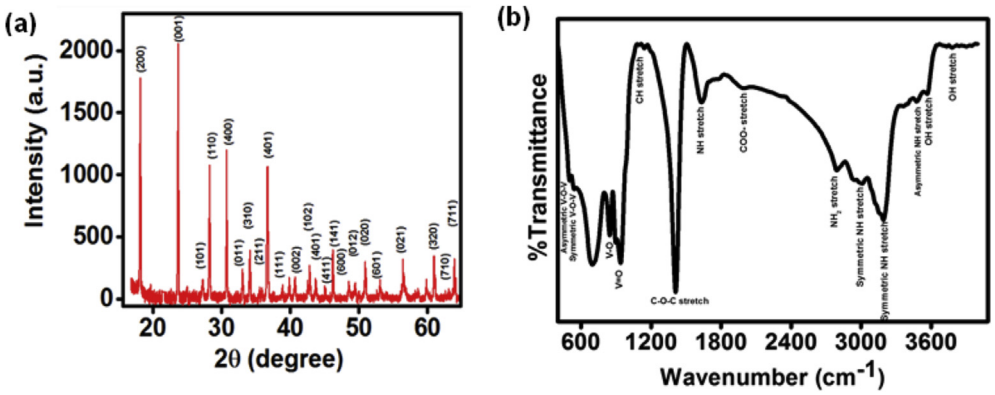

Fig. 2. (a) XRD pattern of V_2O_5 nanoparticles and (b) FT-IR spectrum of V_2O_5/GSH/Chitosan.

Diffraction Standards (JCPDS) card number 41-1426.

FT-IR study

FT-IR spectrum of V_2O_5/GSH/Chitosan is shown in Fig. 2(b). The presence of V_2O_5 nanoparticles was confirmed by the absorption bands at 542 cm^{-1} (symmetric V-O-V), 503 cm^{-1} (asymmetric V-O-V), 846 cm^{-1} (V-O type), and 939 cm^{-1} (V=O type). The absorption bands at 1411 cm^{-1} (C-O-C stretch), 1142 cm^{-1} (CH stretch), 1096 cm^{-1} (CO stretch), 2792 cm^{-1} (NH_2 stretch) and 3780 cm^{-1} (OH stretch) were observed due to the presence of chitosan. Also, the absorption bands at 1632 cm^{-1} (NH stretch), 1997 cm^{-1} (COO^- stretch) 3011 cm^{-1} and 3191 cm^{-1} (symmetric NH stretch), 3476 cm^{-1} (asymmetric NH stretch), 3566 cm^{-1}, 3734 cm^{-1} and 3902 cm^{-1} (OH stretch) formed due to the presence of GSH. The obtained results confirmed the immobilization of chitosan and GSH on V_2O_5 nanoparticles.

Electrochemical behavior of various modified Pt electrodes

Cyclic voltammetric responses of bare Pt, Pt/GSH/Chitosan and Pt/V_2O_5/GSH/Chitosan in the absence and presence of 0.1 μM MG in 0.1 M PBS (PH 7.4) at a scan rate of 1 mV s^{-1} are shown in Fig. 3. Comparison of electrochemical parameters for various modified Pt working electrodes are given in Table 1. No significant redox peak current density was noticed at bare Pt electrode, suggesting the inability of Pt electrode to electrocatalyse MG to hemithioacetal. When the cyclic voltammograms of Pt/GSH/Chitosan and Pt/V_2O_5/GSH/Chitosan were recorded in the absence of MG, the redox peak current densities were clearly decreased. On the other hand, cyclic

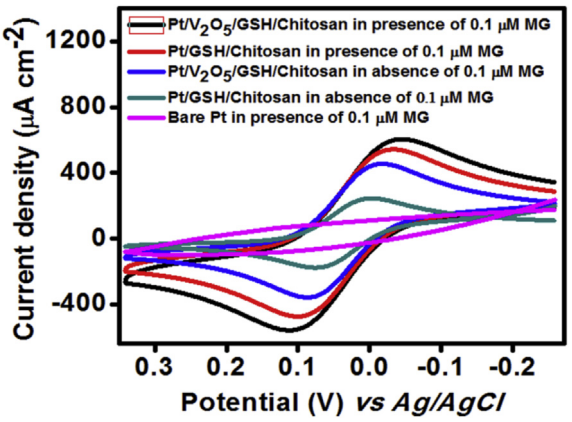

Fig. 3. Cyclic voltammograms of bare Pt, Pt/GSH/Chitosan and Pt/V_2O_5/GSH/Chitosan in the absence and presence of 0.1 μM MG in 0.1 M PBS (pH 7.4) at a scan rate of 1 mV s^{-1}.

voltammograms of Pt/GSH/Chitosan and Pt/V_2O_5/GSH/Chitosan in the presence of MG showed a drastic increase in the peak current densities, implying that the electron transfer between the Pt working electrode and immobilized GSH was rapid. This might be also due to the abundant electron transfer site and high surface area of V_2O_5 nanoparticles. Comparing with other modified Pt electrode, the ratio of anodic to cathodic peak current density for Pt/V_2O_5/GSH/Chitosan was greater than 1 with a value of 1.11. It indicated that V_2O_5 nanoparticles transferred a large number of electrons in the anodic process than in the cathodic process.

The MG sensing mechanism at the surface of Pt/GSH/Chitosan is given as follows: (i) In the absence of MG, Pt/GSH/Chitosan bioelectrode oxidized GSH to GSSG at −2.74 mV, which was then subjected to cathodic reduction at 77.37 mV (*vs Ag/AgCl*). (ii) The oxidized GSSG reduced at 77.37 mV (*vs Ag/AgCl*) to form GSH resulting in two electron transfer in the Pt/GSH/Chitosan bioelectrode.

$$2GSH \leftrightharpoons GSSG + 2H^+ + 2e^-$$

In the presence of 0.1 μM MG, the reduced glutathione got oxidized to GSSG at an applied potential of −32.29 mV (*vs Ag/AgCl*), which further reacted with MG at an applied potential of 93.28 mV (*vs Ag/AgCl*) to form hemithioacetal. The similar trend was also observed at Pt/V_2O_5/GSH/Chitosan bioelectrode.

$$2GSH \rightarrow GSSG + 2H^+ + 2e^-$$

$$(CH_3C(O)CHO) + GSSG + 2H^+ + 2e^- \rightarrow CH_3COCH(OH) - SG$$

The peak to peak separations (ΔE_p) observed at the cyclic voltammogram of various modified Pt bioelectrodes in the absence and presence of MG were greater than 60 mV, which revealed the quasi-reversible electron transfer process. Comparing with Pt/GSH/Chitosan bioelectrode (ΔE_p = 125.57 mV), only the change in peak potential separation of Pt/V_2O_5/GSH/Chitosan bioelectrode (ΔE_p = 158.81 mV) was larger, which can be attributed to the different orientation of immobilized GSH biomolecule on V_2O_5 nanoparticles.

The values of electron transfer rate constant ($K_s = \frac{I_p}{Q}$, where, Q is the amount of charge consumed and I_p the peak current) of the Pt/GSH/Chitosan and Pt/V_2O_5/GSH/Chitosan bioelectrodes in the presence of MG were estimated as 2.14, 3.85 s^{-1} in the cathodic process and 1.85, 3.52 s^{-1} in the anodic process respectively. These values were smaller than that of the Pt/GSH/Chitosan (1.25 and 1.37 s^{-1} in cathodic and anodic process respectively) and Pt/V_2O_5/GSH/Chitosan (1.87 and 2.53 s^{-1} in cathodic and anodic process respectively) in the absence of MG. All the above results manifested that the presence of V_2O_5 nano-interface enhanced the electron transfer rate between the immobilized GSH co-factor and Pt working electrode surface.

The surface coverage (Γ) of the adsorbed electroactive MG biomolecule on the modified Pt working electrode was calculated according to the equation (Eq. (1)),

$$\Gamma = \frac{I_p(irrev.)2.718\ RT}{n\alpha n_\alpha F^2 A\ V} \quad (1)$$

where, F is the Faraday constant, α is the charge transfer coefficient, T is the room temperature, n_α is the number of electron involved in the charge transfer step, Γ is the surface density of the adsorbed MG, I_p (irrev.) is the irreversible peak current, R is the gas constant, V is the scan rate, n is the number of electrons involved in the redox reaction and A is the area of the Pt working electrode. As given in Table 1, the surface coverage value of adsorbed electroactive MG on the Pt/V_2O_5/GSH/Chitosan bioelectrode (28.95 × 10^{-9} M cm^{-2} in the anodic process and 24.89 × 10^{-9} M cm^{-2} in cathodic process) was higher than that of adsorbed electroactive MG on Pt/GSH/Chitosan (22.15 × 10^{-9} M cm^{-2} in the anodic process and 20.54 × 10^{-9} M cm^{-2} in cathodic process) bioelectrode. The enhanced surface coverage of adsorbed electroactive MG might be due to the high surface area of V_2O_5 nanoparticles.

Influence of scan rate on the electrochemical behaviour of Pt/V_2O_5/GSH/Chitosan

Fig. 4(a) shows the cyclic voltammograms of Pt/V_2O_5/GSH/Chitosan bioelectrode recorded at various scan rates ranging from 1 to 10 mV s^{-1}. As can be seen from Fig. 4(b), both the cathodic and anodic current densities were dependent on the applied scan rate. Both the anodic (J_{pa} = 36165.57 [υ] + 142.91, R^2 = 0.99) and cathodic peak current densities (J_{pc} = −43952.96 [υ] - 133.50, R^2 = 0.99) increased linearly with an increase in scan rate from 1 to

Table 1
Electrochemical parameters estimated for the different modified Pt electrodes.

Electrode	ΔE_p (mV)	J_{pc} (μA cm^{-2})	J_{pa} (μA cm^{-2})	E_{pc} (mV)	E_{pa} (mV)	Cathode K_s (s^{-1})	Anode K_s (s^{-1})	Cathode Γ (×10^{-9} M cm^{-2})	Anode Γ (×10^{-9} M cm^{-2})
Pt/GSH/Chitosan (absence of MG)	80.11	208.58	187.55	77.37	−2.37	1.25	1.37	9.58	10.25
Pt/V_2O_5/GSH/Chitosan (absence of MG)	103.41	405.78	402.56	85.89	−17.52	1.87	2.53	10.24	11.68
Pt/GSH/Chitosan (presence of MG)	125.57	501.3	486.11	93.28	−32.29	2.14	1.85	20.54	22.15
Pt/V_2O_5/GSH/Chitosan (presence of MG)	158.81	594.2	554.47	111.75	−47.06	3.85	3.52	24.89	28.95

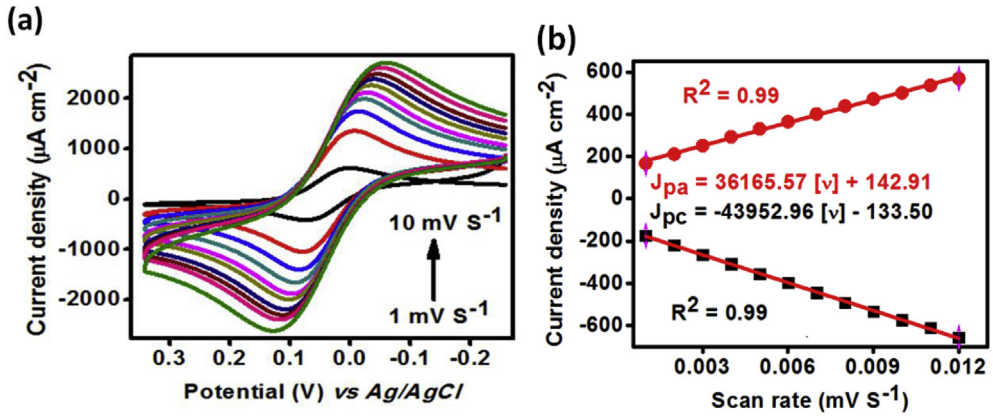

Fig. 4. (a) Cyclic voltammograms of Pt/V_2O_5/GSH/Chitosan bioelectrode recorded at various scan rates ranging from 1 to 10 mV s^{-1} and (b) a plot of peak current density *vs* scan rate.

10 mV s^{-1}. These results indicated that the nature of redox process was controlled by surface confined electroactive MG biomolecules adsorbed onto the surface of Pt/V_2O_5/GSH/Chitosan bioelectrode. Shift in peak potentials was observed with an increase in the scan rate revealed the electroactive MG adsorption complications at the surface of Pt/V_2O_5/GSH/Chitosan bioelectrode.

Effect of methylglyoxal

Cyclic voltammetric curves of Pt/V_2O_5/GSH/Chitosan bioelectrode for increasing MG in 0.1 M PBS (pH 7.4) at 10 mV s^{-1} are shown Fig. 5(a). The peak current density of Pt/V_2O_5/GSH/Chitosan bioelectrode increased (J_{pa} = 1726.12 [MG] + 18.45, R^2 = 0.99 and J_{pc} = 1130.86 [MG] + 22.95, R^2 = 0.99) with an increase in the MG concentration ranging from 0.1 to 100 μM (Fig. 5(b)). This increase in redox current density might be due to the enhanced binding of electroactive MG to the immobilized GSH. Maximum current density (J_{max}) and Michaelis-Menten constant (K_M) were calculated from the Hanes-Woolf plot. The J_{max} and K_M determined from Hanes-Woolf plot were 1608.02 μA cm^{-2} and 0.65 μM respectively. From the Hanes-Woolf plot, it was observed that immobilized GSH in the developed Pt/V_2O_5/GSH/Chitosan bioelectrode showed good affinity to MG. The low K_M also depicted that the diffusion of electroactive MG through the chitosan membrane was much easier in the Pt/V_2O_5/GSH/Chitosan bioelectrode.

The minimal signal required to detect MG can be calculated using limit of detection (LOD) and limit of quantification (LOQ) was calculated using the equations (Eq. (2) and (3)),

$$LOD = 3 \times \frac{s_b}{S} \quad (2)$$

$$LOQ = 10 \times \frac{s_b}{S} \quad (3)$$

where, s_b is the standard deviation in the absence of MG and S is the slope of calibrated curve in the presence of MG. LOD and LOQ for the Pt/V_2O_5/GSH/Chitosan bioelectrode were found to be 2 nM and 6.6 nM respectively. The response time of the developed MG biosensor was found to be ≤ 18 s. Such a low response time was due to the enhanced electron transfer rate provided by V_2O_5 nano-interface.

Accuracy

The accuracy of Pt/V_2O_5/GSH/Chitosan bioelectrode was evaluated using 0.01, 0.5 and 5 μM of MG in 0.1 M PBS (pH 7.4). For 0.01, 0.5 and 5 μM of MG, mean MG detected ± relative error for 4 trials were 0.01 ± 0.002, 0.5 ± 0.01, 5 ± 0.001 μM respectively.

Precision

Repeatability and reproducibility of Pt/V_2O_5/GSH/Chitosan

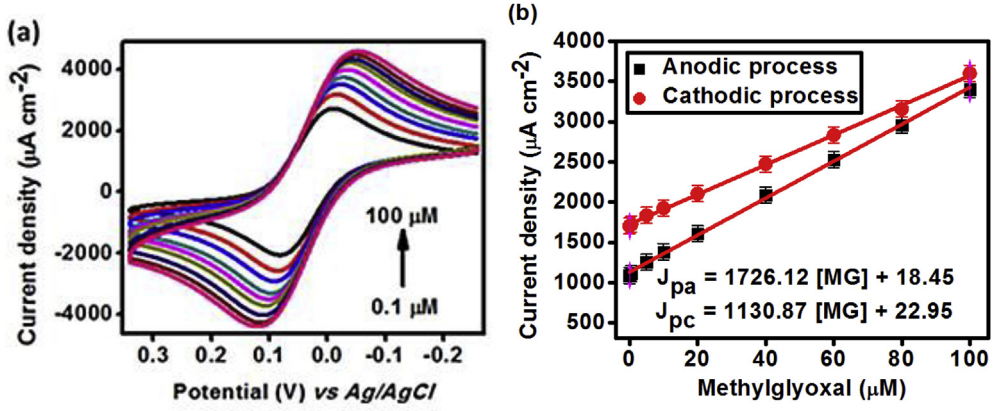

Fig. 5. (a) Cyclic voltammograms of Pt/V_2O_5/GSH/Chitosan bioelectrode for increasing MG in 0.1 M PBS (pH 7.4) at 10 mV s^{-1} and (b) calibration plots of peak current density *vs* [MG].

Table 2
Recovery studies of MG in raw and par-boiled rice samples.

Sample	Total spiked MG (Added MG in each case) (μM)	Total predicted MG (predicted MG in raw rice + predicted MG after spiking) (μM)	Recovery (%)	RSD (%)
Raw rice	0 (0)	0.01 (0.01 + 0)	–	–
	0.3 (0.3)	0.29 (0.01 + 0.28)	95	3.62
	0.4 (0.1)	0.67 (0.01 + 0.66)	95	3.62
	0.6 (0.2)	1.26 (0.01 + 1.25)	98	1.18
	0.8 (0.2)	2.05 (0.01 + 2.04)	98	0.88
Sample	**Total spiked MG** (Added MG in each case) **(μM)**	**Total predicted MG** (predicted MG in par-boiled rice + predicted MG after spiking) **(μM)**	**Recovery (%)**	**RSD (%)**
Par boiled rice	0 (0)	0.12 (0.12 + 0)	–	–
	0.2 (0.2)	0.33 (0.12 + 0.21)	105	3.44
	0.4 (0.2)	0.75 (0.12 + 0.63)	105	3.44
	0.6 (0.2)	1.33 (0.12 + 0.21)	98.66	2.39
	0.8 (0.2)	2.12 (0.12 + 1.0)	98.75	0.88

bioelectrode with 0.01 μM MG in 0.1 PBS (pH 7.4) for intra-assay and inter-assay were carried out for 5 times and the obtained results were analyzed using relative standard deviation (RSD). The RSD of intra-assay and inter-assay was estimated as 1.2% and 0.7% respectively. These results indicated that binding between immobilized GSH co-factor V_2O_5 nanoparticles was good.

Interferent studies

Ascorbic acid (0.1 mM), uric acid (0.1 mM), lactic acid (0.1 mM) and glucose (0.1 mM) were the common interferents used in the interferent studies because they have the significant effect in reducing the catalytic activity of GSH. The concentrations of these interferents were taken at the higher level than the normal level in raw and par-boiled rice samples. Percentage Inhibition (%Inhibition) was calculated using equation (Eq. (4)),

$$I\% = \frac{I_0 - I_i}{I_0} \times 100 \quad (4)$$

where, I_i is the obtained current in the presence of inhibitor and I_0 is the obtained current in the absence of inhibitor. Even at the high interferent concentration used in the study, only 0.72–1.73% degree of inhibition was observed, which confirmed the good specificity of immobilized GSH co-factor towards MG.

Stability studies

The stability of Pt/V_2O_5/GSH/Chitosan bioelectrode was calculated using equation (Eq. (5)),

$$\%\ \text{Stability} = 100 - \left[\frac{J_n - J_0}{J_0}\right] \quad (5)$$

where, J_n is the measured current density in the 'n' day and J_o is the measured current density in the first day. The dry stability of the developed Pt/V_2O_5/GSH/Chitosan bioelectrode was checked for 20 days at room temperature retained approximately 92% of its original activity. The increase in stability was due to the biocompatible environment provided by V_2O_5 nanoparticles around the immobilized GSH.

Determination of methylglyoxal in rice samples

Results for the quantification of MG in rice samples such as raw rice and par-boiled rice are given in Table 2. In order to study the practicability of the developed Pt/V_2O_5/GSH/Chitosan bioelectrode, a recovery test was conducted on the rice samples with four levels of determination: 0.2, 0.4, 0.6 and 0.8 μM. In this recovery study, the quantified MG concentrations were compared with added MG concentrations. The concentrations of MG in raw and par-boiled rice samples were estimated to be 0.01 μM and 0.12 μM respectively. The recovery values of MG in raw rice and par-boiled rice samples were ranging from 95% to 105%. These recovery results showed that the potential interferent in the rice samples didn't interfere the quantification of MG. It also indicated that the developed bioelectrode was accurate. The RSD of MG in raw rice and par-boiled rice samples was in range of 0.88–3.62%, which confirmed the good repeatability and reproducibility of the developed Pt/V_2O_5/GSH/Chitosan bioelectrode.

The performance of the developed MG biosensor in this work was compared with other reported MG biosensors. It is apparent from Table 3 that the Pt/V_2O_5/GSH/Chitosan bioelectrode possessed swift response time and higher sensitivity.

Conclusion

A novel approach for the detection of MG in rice samples using V_2O_5 nano-interface modified Pt electrode was developed.

Table 3
Comparison of performance of the developed MG biosensor with other MG biosensors.

Sample	Electrode matrix	Sensitivity (μA μM^{-1})	Reproducibility (%RSD)	Response time (s)	Linear range (μM)	Reference
Beer/wine	GCE/Pt/SWCNT	0.114	1.95	–	0.1–100	[4]
Human plasma	GCE/SWCNT	0.076	2.76	–	0.1–100	[5]
Human blood	Pt/ZnO/GLO 1/Chitosan	0.022	6.54	–	0.2–100	[6]
Grilled chicken	Pt/ZnO/GLO 1/Chitosan	2.615	5.564	–	0.2–100	[7]
Cow milk	Pt/CeO_2/GLO 1/Chitosan	2.347	1.34	<40	5–50	[3]
Rice	Pt/V_2O_5/GSH/Chitosan	35.51	1.2	<18	0.1–100	Present work

Significantly, the modified Pt electrode showed an excellent electrocatalytic activity towards the oxidation of GSH to GSSG and the reduction of MG to hemithioacetal respectively. The specificity was attained using GSH as a co-factor. The synthesized V_2O_5 nanoparticles enhanced the electron transfer rate between GSH and Pt electrode. The developed Pt/V_2O_5/GSH/Chitosan bioelectrode exhibited a response time of <18 s, stability of 92% (20 days) with LOD and LOQ of 2 nM and 6.6 nM respectively. This work could be further extended towards the detection of MG in the variety of rice samples.

Acknowledgements

The authors are grateful to the Department of Science & Technology, New Delhi for their financial support (DST/TM/WTI/2K14/197(a)(G)), (SR/FST/ETI-284/2011 (C)), (SR/FST/LSI-453/2010), and (SR/NM/PG-16/2007). We also acknowledge SASTRA University, Thanjavur for extending infrastructure support to carry out the study.

Appendix A. Supplementary data

Supplementary data related to this article can be found at http://dx.doi.org/10.1016/j.ab.2017.04.010.

References

[1] L. Xia, C. Ti, B. Li, Y. Xia, X. Yan, Greenhouse gas emissions and reactive nitrogen releases during the life-cycles of staple food production in China and their mitigation potential, Sci. Total Environ. 556 (2016) 116–125, http://dx.doi.org/10.1016/j.scitotenv.2016.02.204.

[2] J. Uribarri, S. Woodruff, S. Goodman, W. Cai, X. Chen, R. Pyzik, A. Yong, G.E. Striker, H. Vlassara, Advanced glycation end products in foods and a practical guide to their reduction in the diet, J. Am. Diet. Assoc. 110 (2010) 911–916.e12, http://dx.doi.org/10.1016/j.jada.2010.03.018.

[3] B.L. Ramachandra, S. Vedantham, U.M. Krishnan, N. Nesakumar, J.B. Balaguru Rayappan, Estimation of methylglyoxal in cow milk – an accurate electrochemical response time based approach, Anal. Methods 8 (2016) 2207–2217, http://dx.doi.org/10.1039/C5AY02901E.

[4] M.A.H. Shipar, Formation of pyrazines in hydroxyacetaldehyde and glycine nonenzymatic browning Maillard reaction: a computational study, Food Chem. 103 (2007) 1208–1216, http://dx.doi.org/10.1016/j.foodchem.2006.10.025.

[5] M.P. Kalapos, Where does plasma methylglyoxal originate from? Diabetes Res. Clin. Pract. 99 (2013) 260–271, http://dx.doi.org/10.1016/j.diabres.2012.11.003.

[6] S. Ogawa, K. Nakayama, M. Nakayama, T. Mori, M. Matsushima, M. Okamura, M. Senda, K. Nako, T. Miyata, S. Ito, Methylglyoxal is a predictor in type 2 diabetic patients of intima-media thickening and elevation of blood pressure, Hypertension 56 (2010) 471–476, http://dx.doi.org/10.1161/HYPERTENSIONAHA.110.156786.

[7] M. Brownlee, The pathobiology of diabetic complications: a unifying mechanism, Diabetes 54 (2005) 1615–1625, http://dx.doi.org/10.2337/diabetes.54.6.1615.

[8] J. Zhang, H. Zhang, M. Li, D. Zhang, Q. Chu, J. Ye, A novel capillary electrophoretic method for determining methylglyoxal and glyoxal in urine and water samples, J. Chromatogr. A. 1217 (2010) 5124–5129, http://dx.doi.org/10.1016/j.chroma.2010.05.040.

[9] S. Chatterjee, A. Chen, Voltammetric detection of the dicarbonyl compound: methylglyoxal as a flavoring agent in wine and beer, Anal. Chim. Acta 751 (2012) 66–70, http://dx.doi.org/10.1016/j.aca.2012.09.011.

[10] S. Chatterjee, J. Wen, A. Chen, Electrochemical determination of methylglyoxal as a biomarker in human plasma, Biosens. Bioelectron. 42 (2013) 349–354, http://dx.doi.org/10.1016/j.bios.2012.10.091.

[11] S. Grassino, Antonela Nincevic Milardovic, Z. Grabaric, B.S. Grabaric, Amperometric assessment of glucose electrode behaviour in mixed solvents and determination of glucose in dairy products, Food Chem. 125 (2011) 1335–1339, http://dx.doi.org/10.1016/j.foodchem.2010.10.001.

[12] A. Thangavel, S. Alagesan, N. Nesakumar, B.L. Ramachandra, M.B. Gumpu, S. Vedantham, S. Sethuraman, U.M. Krishnan, J.B.B. Rayappan, Optimization of electrochemical parameters for specific blood methylglyoxal determination using ZnO sepals based glyoxalase 1 biosensor, Sens. Lett. 13 (2015) 328–337, http://dx.doi.org/10.1166/sl.2015.3439.

[13] M. Ezhilan, S. Alagesan, B.L. Ramachandra, M.B. Gumpu, N. Nesakumar, S. Vedantham, S. Sethuraman, U.M. Krishnan, J.B.B. Rayappan, Chemometric analysis for the determination of methylglyoxal in grilled chicken using ZnO flakes based glyoxalase 1 biosensor, Sens. Lett. 13 (2015) 245–253, http://dx.doi.org/10.1166/sl.2015.3425.

[14] J. Pan, M. Li, Y. Luo, H. Wu, L. Zhong, Q. Wang, G. Li, Microwave-assisted hydrothermal synthesis of V2O5 nanorods assemblies with an improved Li-ion batteries performance, Mater. Res. Bull. 74 (2016) 90–95, http://dx.doi.org/10.1016/j.materresbull.2015.10.020.

[15] V.S. Patil, P.R. Gogate, Ultrasound-assisted improved synthesis of supported V2O5 catalyst and subsequent application for the production of n-hexyl acetate, Chem. Eng. J. 289 (2016) 513–524, http://dx.doi.org/10.1016/j.cej.2016.01.015.

[16] S. Balasubramanian, K.K. Purushothaman, Carbon coated flowery V2O5 nanostructure as novel electrode material for high performance supercapacitors, Electrochim. Acta 186 (2015) 285–291, http://dx.doi.org/10.1016/j.electacta.2015.10.160.

[17] Q. Zhen, L. Li, R. Li, F. Lu, Z. Li, Y. Wang, Morphology controllable preparation and infrared emissivity of vanadium pentoxide, Infrared Phys. Technol. 71 (2015) 303–306, http://dx.doi.org/10.1016/j.infrared.2015.05.003.

[18] H.T. Chiang, T.-M. Chen, Synthesis and characterization of single-crystalline vanadium pentoxide by the low-temperature of glycothermal method, Mater. Lett. 157 (2015) 205–208, http://dx.doi.org/10.1016/j.matlet.2015.05.112.

[19] Y.B. Kim, M.W. Shin, Synthesis of diverse structured vanadium pentoxides particles by the simplified hydrothermal method, Mater. Lett. 132 (2014) 247–250, http://dx.doi.org/10.1016/j.matlet.2014.06.086.

[20] D. Su, S. Dou, G. Wang, Hierarchical vanadium pentoxide spheres as high-performance anode materials for sodium-ion batteries, Chem. Sus. Chem. 8 (2015) 2877–2882, http://dx.doi.org/10.1002/cssc.201500139.

[21] P.R. Solanki, A. Kaushik, V.V. Agrawal, B.D. Malhotra, Nanostructured metal oxide-based biosensors, NPG Asia Mater 3 (2011) 17–24, http://dx.doi.org/10.1038/asiamat.2010.137.